Solid State Phenomena Vol. 160 (2010) pp 47-54
© (2010) Trans Tech Publications, Switzerland
doi:10.4028/www.scientific.net/SSP.160.47

Texture heterogeneity in ECAP deformed copper

W. Skrotzki[1,a], C. Tränkner[1,b], R. Chulist[1,c], B. Beausir[1,d], S. Suwas[2,e] and L. S. Tóth[3,f]

[1]Institut für Strukturphysik/Professur für Metallphysik, Technische Universität Dresden, D-01062 Dresden, Germany

[2]Lehrstuhl Allgemeine Werkstoffeigenschaften, Universität Erlangen-Nürnberg, Martensstr. 5, D-91058 Erlangen, Germany

[3] LPMM, Université Paul Verlaine de Metz, Ile du Saulcy, F-57045 Metz, France

[a] werner.skrotzki@physik.tu-dresden.de, [b] christine.traenkner@physik.tu-dresden.de, [c] robert.chulist@physik.tu-dresden.de, [d] b.beausir@physik.tu-dresden.de, [e] satyamsuwas@materials.iisc.ernet.in, [f] laslo.toth@univ-metz.fr

Keywords: Copper, equal channel angular pressing (ECAP), route B_C, texture, heterogeneity

Abstract. Polycrystalline copper of 4N purity has been deformed by equal channel angular pressing at room temperature using route B_C. Local textures have been measured by high-energy synchrotron radiation along 3 lines in the cross section from the top to the bottom of the billets. The texture heterogeneity observed in the cross section is presented for 2 passes and discussed with regard to friction-affected material flow.

Introduction

Equal channel angular pressing (ECAP) is the most frequently used method of severe plastic deformation producing submicro- to nanocrystalline metals and alloys [1]. Such advanced materials possess extraordinary properties like high strength paired with a moderate ductility [1]. ECAP leads to a pronounced texture development [2] giving rise to anisotropy of the mechanical properties. However, because of friction at the channel walls deformation by ECAP is not uniform, resulting in a gradient from the bottom to the top part of the die [3]. Consequently, texture formation is also non-uniform across the channel. This has been clearly shown for route A [3 - 9] and is also demonstrated here for route B_C. In route B_C the billet is rotated by 90° after each pass [1]. Thus, a gradient is also expected in lateral direction. To test this, the local texture has been measured by high-energy synchrotron radiation along 3 lines in the cross section from the top to the bottom of the billets. Similar investigations have been reported by the authors for Ti ECAP deformed 4 passes using route B_C [10].

Experimental details

A billet (9.9 ×9.9 × 60 mm^3) cut by spark erosion from an extruded pure (4N) Cu rod was processed by ECAP in a Zwick 200 kN screw driven machine. The channels of the ECAP die had a square cross section meeting at an angle $\Phi = 90°$. All corners and edges of the die were sharp. To reduce friction within the ingoing channel (10 × 10 mm^2) and thus reducing the pressing force, three walls of the channel were allowed to move with the billet except the front X-wall. On the other hand, friction on the walls of the outgoing channel had been increased by narrowing this channel on each side by 0.1 mm and on the top by 0.2 mm in order to compensate for elastic rebound of the billet after extrusion [11]. Otherwise machining of the billet to the original size is necessary. The ECAP was done at room temperature with a crosshead speed of 1 mms^{-1} using MoS_2 as lubricant. A simplified sketch of the ECAP setup with the coordinate systems is presented in Fig. 1a. ECAP was done via route B_C, i.e. in pass 2 looking in extrusion direction the billet was rotated anticlockwise by 90°. The starting texture of the extruded rod was a <111><100> double fibre texture with <111> dominating [3].

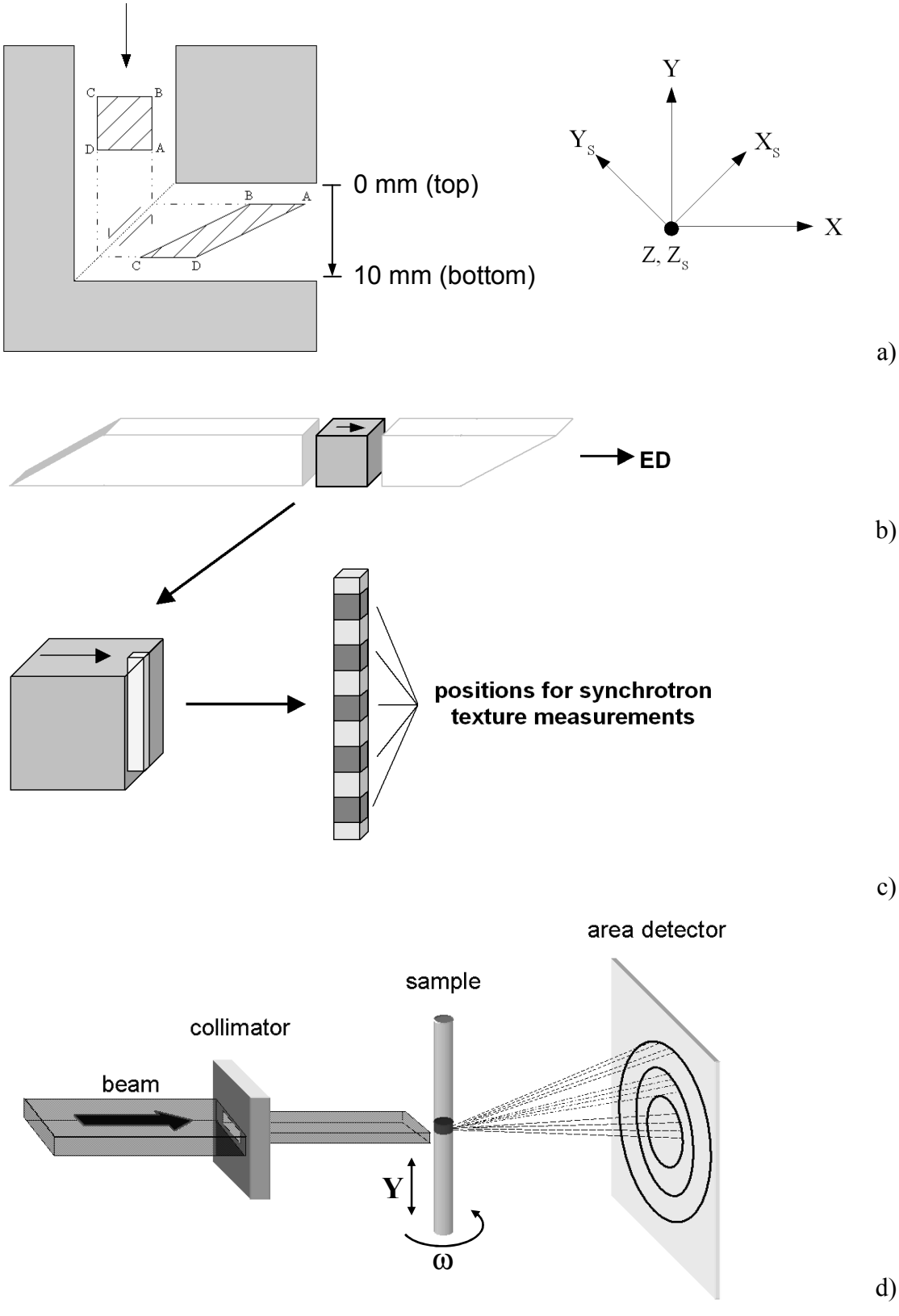

Fig. 1: (a) Volume element ABCD deformed by simple shear in the intersection plane during ECAP and coordinate systems used: X_S, Y_S, Z_S - simple shear system, X, Y, Z - ECAP system, (b) and (c) scheme of sample sectioning for texture measurements with neutrons and synchrotron radiation, respectively, and (d) schematics of texture measurement with synchrotron radiation (simplified).

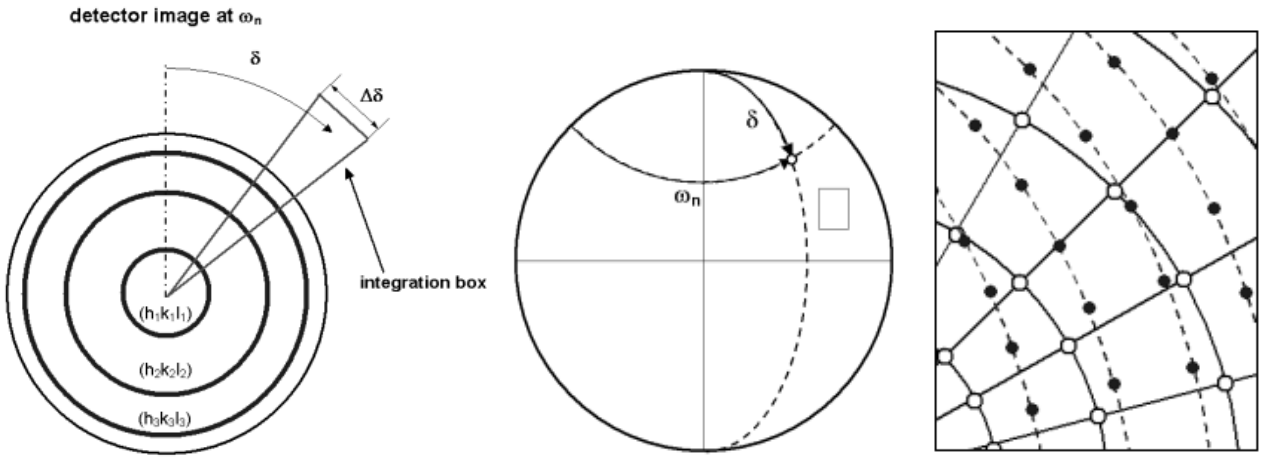

a) b) c)

Fig. 2: Data analysis of texture measurements with synchrotron radiation. (a) Read out of the Debye-Scherrer rings by moving an integration box around the centre of rings in steps δ = 5°. (b) The intensity values of each box Δδ are converted into the corresponding pole figures ($h_ik_il_i$) (simplified sketch for small Bragg angles). The arrows indicate the direction of increasing values of δ and ω_n (ω_n = angle after rotation of n steps of 3° around pin axis). (c) Interpolation on a regular grid: Magnification of the rectangular small area indicated in (b). The original and regular grid are shown by solid and open symbols, respectively

Quantitative texture measurements were performed with high-energy synchrotron radiation at the beamlines BW5 [12, 13] and W2 (≈100 keV) at DESY-HASYLAB (Hamburg, Germany). Synchrotron radiation opens the possibility to investigate small sample volumes of pins taken along the texture gradient (local studies) of ECAP deformed samples (Fig. 1c). In the present study the incident monochromatic beam was defined by a slit system to 3 mm x 0.5 mm.

The small pins were mounted parallel to the rotation axis ω (Fig. 1d). An image plate detector (MAR 345) was positioned perpendicular to the incoming beam at a distance from the sample of about 1.3 m. Thus, several Debye-Scherrer rings could be registered simultaneously. The pins were rotated around the ω-axis from 0° to 180° in steps of 3°, resulting in 61 diffraction images.

The Debye-Scherrer rings were transformed into the corresponding pole figures as follows (Fig. 2). In the first step, the intensity along every ring was read out using a pie-piece like integration box (Fig. 2a), which had an angular width of 5°. For each of the Debye-Scherrer rings, all background corrected values of intensity of each pixel in the integration box were summed up. In a second step, the pole figure coordinates for the integration box were calculated according to the procedure given by Wcislak et al. [13] and Bunge and Klein [14]. The intensities of the resulting pole figure points lie on an irregular grid and have to be interpolated onto a regular 5° × 5° grid in order to calculate the orientation distribution function (ODF) (Figs. 2b, c). The interpolation was done in such a way that for every point of the 5° × 5° grid the three nearest neighbours were determined. The distance weighted mean value of the intensities of these three points is assigned to the corresponding grid point. The pole figures were used to calculate the ODF with the texture analysis software LaboTex [15]. The Euler angles were used in Bunge notation [16]. The shear and ECAP sample coordinate systems are defined in Fig. 1a. Because of triclinic sample symmetry in route B_C the ODF representations are extended to $\varphi_1 = 360°$.

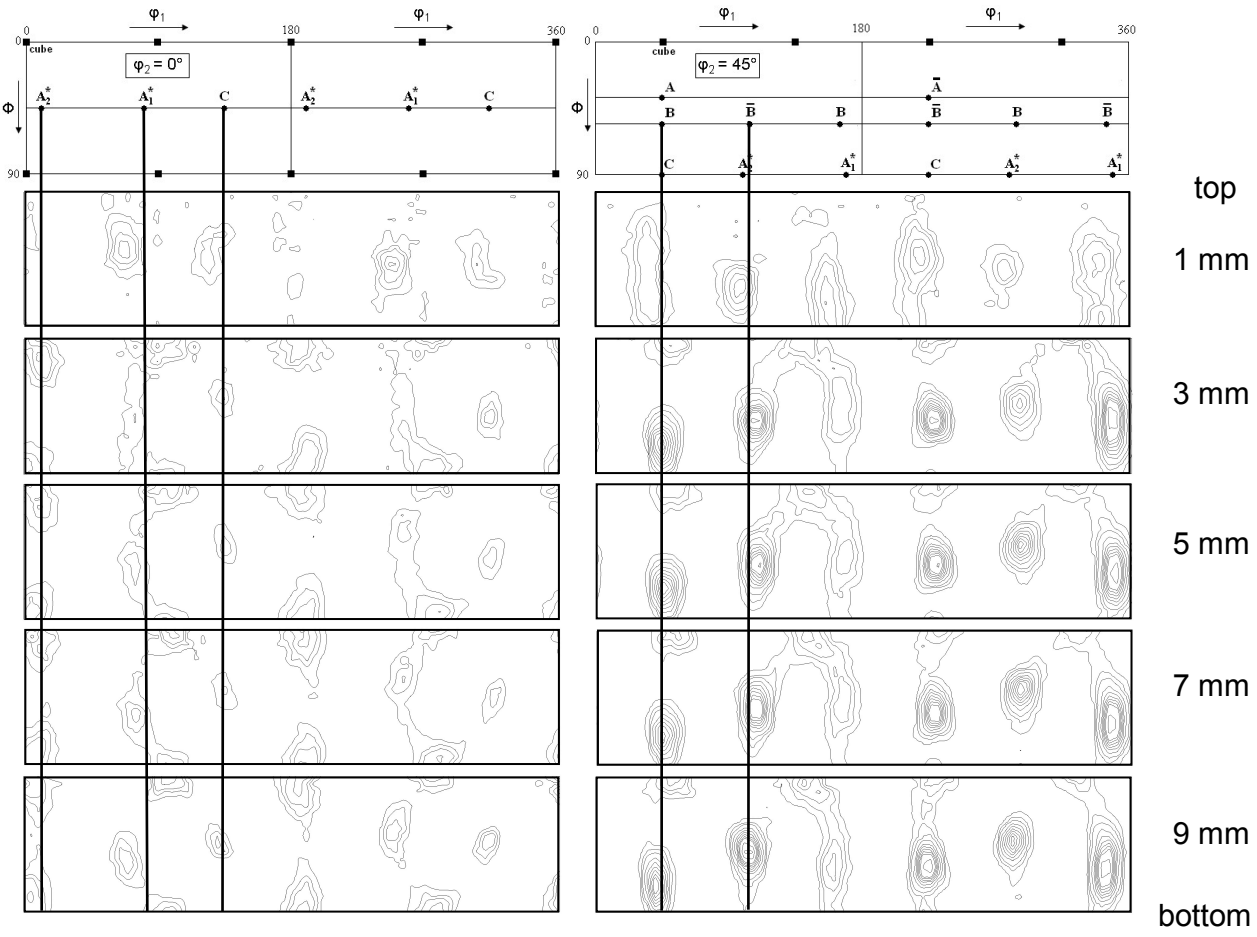

Fig. 3: Local texture after 2 passes of route B_C measured in the middle pin of the billet cross section represented in ODF sections at φ_2 = 0° and 45° (Intensities in mrd: 1, 2, 3, 5, 7, 9, 11, 13, 15, 20, 25, 30). The ideal shear components transferred to the ECAP reference system are given in the key figure.

Results and discussion

The evolution of the texture after 2 passes of route B_C in the middle pin is presented in ODF sections at φ_2 = 0° and 45° in Fig. 3. These sections are sufficient to show the main texture components developing during simple shear in face-centred cubic metals. The positions of the ideal shear components plus cube component in the ODF sections are shown in the key figure. It is evident that the main shear components exist after 2 passes, but they exhibit different intensities. Moreover, the intensities as well as the deviations from the ideal positions change from the top to the bottom of the billet. A quantitative description of the intensities and the deviations in φ_1 are given in Figs. 4 and 5 together with a comparison to passes 1 and 2 of route A [3].

The main results may be summarized as follows:

i) During pass 1, which is the same for both routes, C and A_1^* are the main texture components followed by $B/\overline{B}$ (Fig. 4d). After 2 passes of route A, C decreases while A_1^* and $B/\overline{B}$ slightly increase (Fig. 4e). The texture intensity is quite homogeneous except in the lower quarter of the billet where it slightly decreases. More details are already published in [3]. In contrast, after pass 2 of route B_C $B/\overline{B}$ is dominating with a pronounced intensity (Figs. 4a - c). In addition, there is a gradient from left to right in the billet. While in the middle pin $B/\overline{B}$ almost have the same intensity and show the same trend from top to bottom, on the left and right side the same trend only holds for B and $\overline{B}$, respectively. The corresponding other $B/\overline{B}$ component after a maximum at 3 mm from the top significantly decreases. In all cases, there is a lower intensity in the upper quarter of the billet.

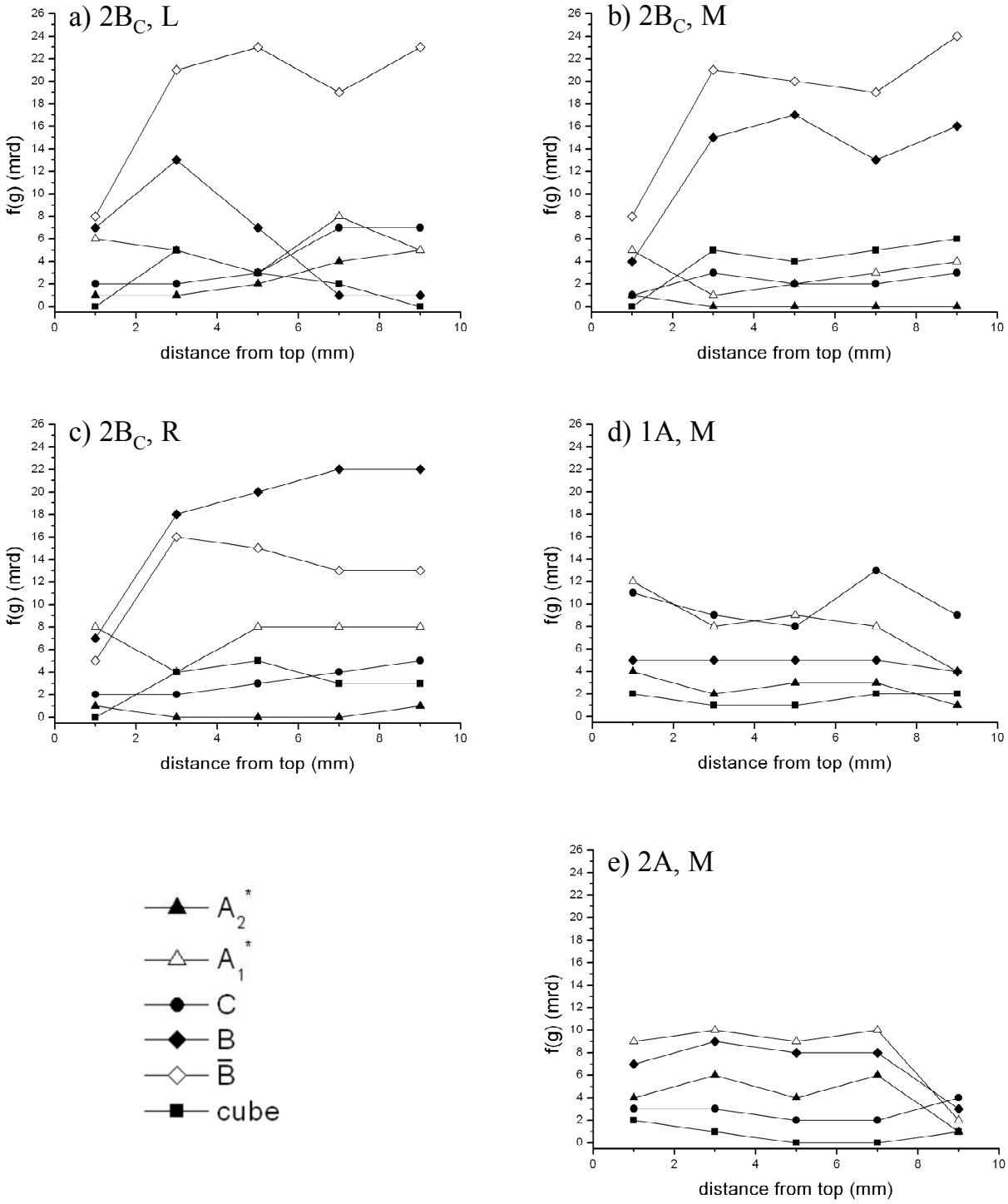

Fig. 4: Change of the texture intensity of the different components for all 3 pins (left side L (a), middle M (b) and right side R (c) of the cross section) from the top to the bottom of the billet processed by route B_C. The middle pin is compared with that of passes 1 (d) and 2 (e) of route A.

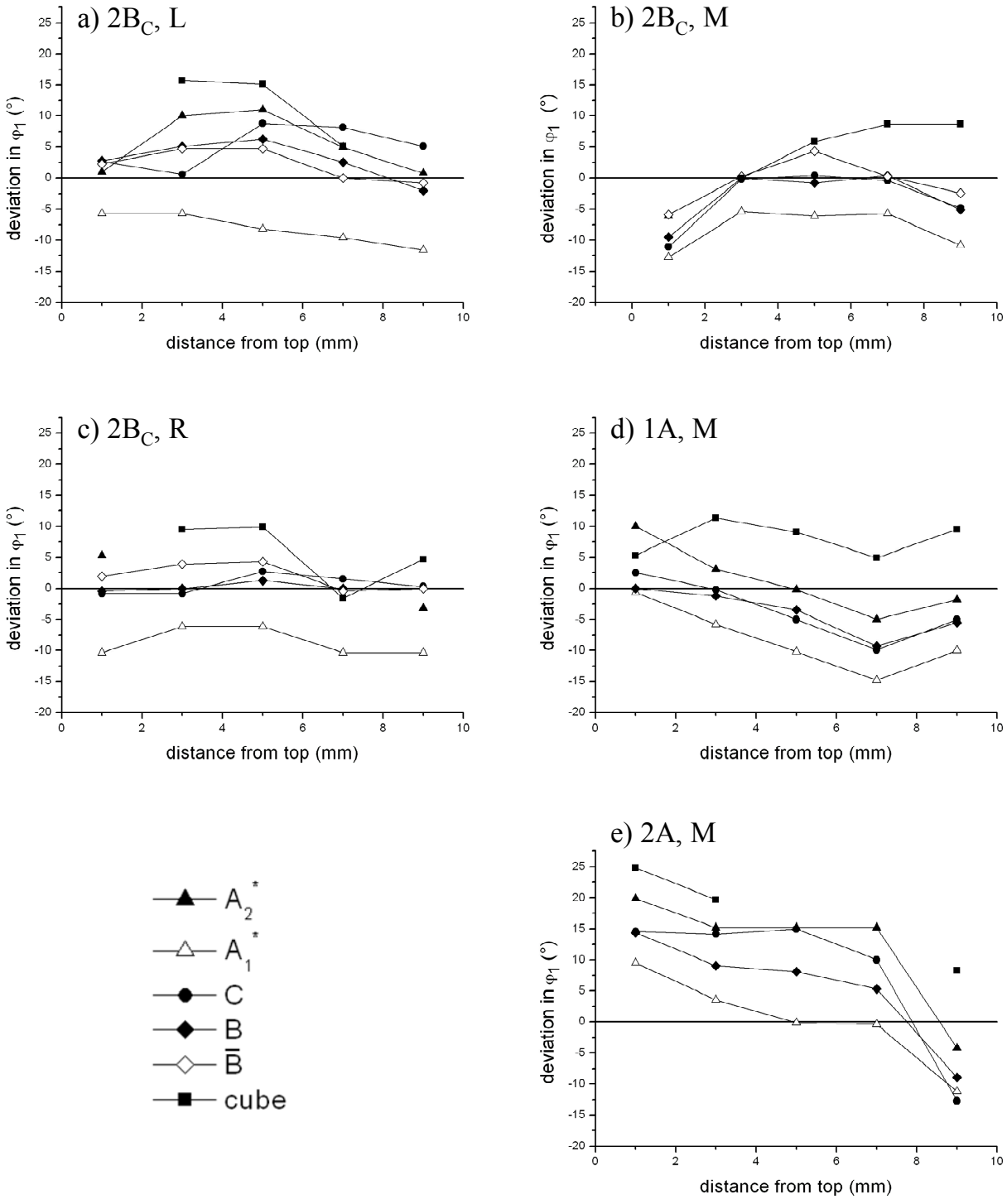

Fig. 5: Change of the deviation in φ_1 of the different components from the ideal positions for all 3 pins (left side L (a), middle M (b) and right side R (c) of the cross section) from the top to the bottom of the billet. The middle pin is compared with that of passes 1 (d) and 2 (e) of route A.

ii) With respect to the deviation in φ_1 from the ideal texture components in pass 1, there is a continuous decrease of all components from positive to negative values (Fig. 5d). The gradient disappears in pass 2 of route A (Fig. 5e). The situation is different and more complex in the lower quarter of the billet. For more information see also [3]. In the case of pass 2 of route B_C the deviations are quite constant between 3 and 7 mm from the top, while in the rest they generally deviate, mostly to lower positive, respectively negative values. In all cases, the deviation sequence of the components is the same with A_1* always displaced to negative angles.
iii) Also included in Figs. 4 and 5 is the cube component. While in general their intensity is quite low, its deviation in φ_1 from the ideal position is maximum in positive direction.

In [3] the texture gradient developing in route A has been successfully explained with the help of Tóth's flow line model [17, 18]. The same arguments should also hold for pass 2 of route B_C, simulations are under way. Interesting is the low intensity of the dominating $B/\overline{B}$ component in the top quarter of the billet independent of the pin and the variation of the B and $\overline{B}$ intensities in lateral direction.

In [19] the rotated cube component has been clearly attributed to dynamic recrystallization. To check this, investigations of the microstructure are under way.

Conclusions

Measurements of the local texture in the cross section of a billet deformed 2 passes by ECAP using route B_C show that there not only exists a texture gradient along the Y (top to bottom) but also along the Z (lateral) direction. The main texture component, B, half way from the top decreases from left to right while $\overline{B}$ shows the opposite trend. Moreover, the rotation leads to the dominance of the $B/\overline{B}$ components in route B_C instead of A_1^* in route A.

For technical applications of ECAP deformed materials the inhomogeneity of texture and the corresponding non-uniform anisotropy of the mechanical properties should be taken into account.

Acknowledgments

Thanks are due to DESY-HASYLAB for beamtime and financial support of travel and accommodation. The technical assistance by Mr. T. Reiter (TU Dresden) is gratefully acknowledged.

References

[1] R.Z. Valiev and T.G. Langdon: Progress Mater. Sci. Vol. 51 (2006), p. 881.

[2] I. Beyerlein and L.S. Tóth: Progress Mater. Sci. Vol. 54 (2009), p. 427.

[3] W. Skrotzki, N. Scheerbaum, C.-G. Oertel, R. Arruffat-Massion, S. Suwas and L.S. Tóth: Acta Mater. Vol. 55 (2007), p. 2013.

[4] W. Skrotzki, N. Scheerbaum, C.-G. Oertel, H.-G. Brokmeier, S. Suwas and L.S. Tóth: Solid State Phenomena Vol. 105 (2004), p. 327.

[5] W. Skrotzki, N. Scheerbaum, C.-G. Oertel, H.-G. Brokmeier, S. Suwas and L.S. Tóth: Mater. Sci. Forum Vols. 495 - 497 (2005), p. 839.

[6] W. Skrotzki, N. Scheerbaum, C.-G. Oertel, H.-G. Brokmeier, S. Suwas and L.S. Tóth: Mater. Sci. Forum Vols. 503 - 504 (2006), p. 99.

[7] W. Skrotzki, B. Klöden, C.-G. Oertel, R. Arruffat-Massion, S. Suwas and L.S. Tóth: Mater. Sci. Forum Vols. 558 - 559 (2007), p. 575.

[8] W. Skrotzki, L.S. Tóth, B. Klöden, H.-G. Brokmeier and R. Arruffat-Massion: Acta Mater. Vol. 56 (2008), p. 3439.

[9] T. Grosdidier, J.-J. Fundenberger, D. Goran, E. Bouzy, S. Suwas, W. Skrotzki and L.S. Tóth: Scripta mater. Vol 59 (2008), p. 1087.

[10] W. Skrotzki, B. Klöden, A. Lankau, R. Chulist, V. Kopylov and H.-G. Brokmeier: Archives Metall. Mater. Vol. 53 (2008), p. 29.

[11] J.-P. Mathieu, S. Suwas, A. Eberhardt, L.S. Tóth and P.J. Moll: Mater. Processing Technol. Vol. 173 (2006), p. 29.

[12] R. Bouchard, D. Hupfeld, T. Lippmann, J. Neuefeind, H.B. Neumann, H.F. Poulsen, U. Rütt, T. Schmidt, J.R. Schneider, J. Süssenbach and M. von Zimmermann: J. Synchrotron Rad. Vol. 5 (1998), p. 90.

[13] L. Wcislak, H. Klein, H.J. Bunge, U. Garbe, T. Tschentscher and J.R. Schneider: J. Appl. Cryst. Vol. 35 (2002), p. 82.

[14] H.J. Bunge and H. Klein: Z. Metallkunde Vol. 87 (1996), p. 465.

[15] K. Pawlik and P. Ozga: Göttinger Arb. Geol. Paläont. Vol. SB4 (1999).

[16] H.J. Bunge: *Texture Analysis in Materials Science, Mathematical Methods.* Culliver Verlag Göttingen (1993).

[17] L.S. Tóth: Adv. Eng. Mat. Vol. 5 (2003), p. 308.

[18] L.S. Tóth, R. Arruffat Massion, L. Germain, S.C. Baik and S. Suwas: Acta Mater. Vol. 52 (2004), p. 1885.

[19] W. Skrotzki, N. Scheerbaum, C.-G. Oertel, H.-G. Brokmeier, S. Suwas and L.S. Tóth: Acta Mater. Vol. 55 (2007), p. 2211.